Published in final edited form as:

Mol Psychiatry. 2020 September ; 25(9): 2070–2085. doi:10.1038/s41380-018-0344-6.

New roles for dopamine D_2 and D_3 receptors in pancreatic beta cell insulin secretion

Zachary J. Farino[1], **Travis J. Morgenstern**[2], **Antonella Maffei**[3], **Matthias Quick**[2,4], **Alain J. De Solis**[5], **Pattama Wiriyasermkul**[2,6], **Robin J. Freyberg**[1], **Despoina Aslanoglou**[1], **Denise Sorisio**[1], **Benjamin P. Inbar**[2], **R. Benjamin Free**[7], **Prashant Donthamsetti**[2,8], **Eugene V. Mosharov**[2,4,9], **Christoph Kellendonk**[2,4,10], **Gary J. Schwartz**[11], **David R. Sibley**[7], **Claudia Schmauss**[2,4], **Lori M. Zeltser**[5,12], **Holly Moore**[2,13], **Paul E. Harris**[3], **Jonathan A. Javitch**[2,4,10], **Zachary Freyberg**[1,14,*]

[1]Department of Psychiatry, University of Pittsburgh, Pittsburgh, PA, USA

[2]Department of Psychiatry, College of Physicians & Surgeons, Columbia University, New York, NY, USA

[3]Division of Endocrinology, Department of Medicine, College of Physicians & Surgeons, Columbia University, New York, NY, USA

[4]Division of Molecular Therapeutics, New York State Psychiatric Institute, New York, NY, USA

[5]Division of Molecular Genetics, Naomi Berrie Diabetes Center, Columbia University, New York, NY, USA

[6]Current address: Department of Collaborative Research, Nara Medical University, Kashihara, Nara, Japan

[7]Molecular Neuropharmacology Section, National Institute of Neurological Disorders and Stroke, National Institutes of Health, Bethesda, MD, USA

[8]Current address: Department of Molecular and Cell Biology, University of California, Berkeley, CA, USA

[9]Department of Neurology, College of Physicians & Surgeons, Columbia University, New York, NY, USA

[10]Department of Pharmacology, College of Physicians & Surgeons, Columbia University, New York, NY, USA

[11]Departments of Medicine and Neuroscience, Albert Einstein College of Medicine, Bronx, NY, USA

Correspondence should be addressed to freyberg@pitt.edu (Z.F.).

*Lead Contact

Conflict of interest

The authors declare no conflict of interest.

The online version of this article contains supplementary material, which is available to authorized users.

[12]Department of Pathology and Cell Biology, College of Physicians & Surgeons, Columbia University, New York, NY, USA

[13]Division of Integrative Neuroscience, New York State Psychiatric Institute, New York, NY, USA

[14]Department of Cell Biology, University of Pittsburgh, Pittsburgh, PA, USA

Abstract

Although long-studied in the central nervous system, there is increasing evidence that dopamine (DA) plays important roles in the periphery including in metabolic regulation. Insulin-secreting pancreatic β-cells express the machinery for DA synthesis and catabolism, as well as all five DA receptors. In these cells, DA functions as a negative regulator of glucose-stimulated insulin secretion (GSIS), which is mediated by DA D_2-like receptors including D_2 (D2R) and D_3 (D3R) receptors. However, the fundamental mechanisms of DA synthesis, storage, release, and signaling in pancreatic β-cells and their functional relevance *in vivo* remain poorly understood. Here, we assessed the roles of the DA precursor L-DOPA in β-cell DA synthesis and release in conjunction with the signaling mechanisms underlying DA's inhibition of GSIS. Our results show that uptake of L-DOPA is essential for establishing intracellular DA stores in β-cells. Glucose stimulation significantly enhances L-DOPA uptake, leading to increased DA release and GSIS reduction in an autocrine/paracrine manner. Furthermore, D2R and D3R act in combination to mediate dopaminergic inhibition of GSIS. Transgenic knockout mice in which β-cell D2R or D3R expression is eliminated exhibit diminished DA secretion during glucose stimulation, suggesting a new mechanism where D_2-like receptors modify DA release to modulate GSIS. Lastly, β-cell-selective D2R knockout mice exhibit marked postprandial hyperinsulinemia *in vivo*. These results reveal that peripheral D2R and D3R receptors play important roles in metabolism through their inhibitory effects on GSIS. This opens the possibility that blockade of peripheral D_2-like receptors by drugs including antipsychotic medications may significantly contribute to the metabolic disturbances observed clinically.

Introduction

Antipsychotic drugs (APDs) are some of the most widely used psychotropic medications today. Yet, these drugs can also produce profound metabolic disturbances[1, 2]. A key feature of this metabolic dysregulation is impaired glycemic control, which ultimately contributes to the development of systemic insulin resistance and type II diabetes (T2D)[3]. Significantly, emerging evidence suggests that APDs increase diabetes risk independently of class or individual agent[4]. However, the mechanisms underlying these APD-induced metabolic abnormalities are still poorly understood. APDs interact with numerous G protein-coupled receptors (GPCRs) including dopaminergic, serotonergic, adrenergic, muscarinic, and histaminergic receptors[5, 6]. Though the pleiotropic nature of APD-receptor interactions may contribute to their numerous side effects[6], the single unifying property of all clinically effective APDs is their action on dopamine (DA) D_2-like receptors (D_2, D_3 and D_4 receptors)[7]. Thus, elucidating the functional relevance of dopaminergic signaling in metabolism may provide important clues in deciphering mechanisms underlying APD-induced metabolic disturbances.

D_2-like receptors are expressed in the central nervous system (CNS) in striatal and hypothalamic brain regions that mediate appetite and feeding behaviors[8, 9]. More recently, studies showed that D_2 (D2R) and D_3 (D3R) receptors are also expressed peripherally in tissues critical for metabolic regulation, including human and rodent insulin-secreting pancreatic β-cells[10–12]. We and our colleagues have demonstrated that *in vitro* stimulation of these receptors in pancreatic islets and cultured β-cells with either exogenous DA or D2R/D3R agonists inhibited glucose-stimulated insulin secretion (GSIS) as part of an autocrine/paracrine negative feedback circuit[10–12]. Similarly, both rodents and humans treated with the DA precursor L-DOPA demonstrated hyperglycemia *in vivo* as a consequence of decreased GSIS[13–16], further suggesting that DA and potentially D2R/D3R signaling play important roles in mediating GSIS. To date, however, the individual contributions of beta cell D2R and D3R in regulating GSIS have yet to be disentangled definitively since most pharmacological agonists and blockers share affinities for both D2R and D3R[10, 11, 17, 18]. Earlier efforts to discern the respective metabolic roles of these receptors *in vivo* using global D2R and D3R knockout (KO) mice have been challenging since both D2R and D3R are expressed in several CNS and peripheral tissues associated with metabolic regulation[19–21]. Thus, it has been difficult to unambiguously interpret the respective central versus peripheral contributions of these receptors to metabolic regulation[13, 22].

Analogous to CNS DA neurons, pancreatic β-cells possess the capacity for DA biosynthesis and catabolism. Indeed, β-cells express tyrosine hydroxylase (TH), the rate limiting enzyme in DA biosynthesis, which converts tyrosine to L-3,4-dihydroxyphenylalanine (L-DOPA)[23, 24]. Likewise, human and rodent β-cells express aromatic amino acid decarboxylase (AADC) which converts L-DOPA to DA[25] as well as the machinery of monoamine catabolism including monoamine oxidases A and B (MAOA and MAOB, respectively)[26]. We also showed that the vesicular monoamine transporter, VMAT2, required for loading of DA into vesicles, is expressed in these cells[11]. Our recent work suggests that DA and L-DOPA synthesis in the gastrointestinal (GI) tract may provide an important physiological source of pancreatic islet DA[27]. Nevertheless, the precise roles of β-cell DA synthesis/utilization in metabolism and, what role, if any, D2R and D3R signaling plays in these processes remain poorly understood.

Here we employed genetic, biochemical and pharmacological approaches *in vitro* and *in vivo* to examine the dopaminergic system in pancreatic β-cells and its effects on insulin and DA release. Using mouse pancreatic islets and INS-1E cells, a rat β-cell-derived cell line[28], we have characterized the cellular machinery responsible for DA biosynthesis. We show that β-cells rely on uptake of the DA precursor L-DOPA by large neutral amino acid transporters to boost intracellular DA stores and that glucose stimulation not only enhances L-DOPA uptake, but also significantly augments subsequent DA release. We demonstrate that L-DOPA-derived DA inhibits GSIS via β-cell D2R and D3R. We also show that these receptors work in concert to modulate both glucose-stimulated insulin and DA secretion using novel receptor-selective pharmacological tools and tissue-specific transgenic KO animals. Significantly, we describe the first β-cell-selective D2R KO mouse to elucidate D2R's specific contributions to pancreatic β-cell function without potential confounds from D2R deletion in metabolically-relevant CNS regions including hypothalamus[29]. Our results

suggest an important role for pancreatic D2R in regulating the coupling between food intake, which provides dietary DA, and peripheral DA signaling and insulin release. These findings establish a new context for studying metabolic regulation by DA D_2-like receptors and may explain how actions on these peripheral targets by APDs can contribute to development of metabolic disturbances.

Materials and Methods

Compounds

Compounds used in this study were purchased from Sigma-Aldrich (St. Louis, MO) unless indicated otherwise: HEPES, sodium pyruvate, penicillin, streptomycin, 2-mercaptoethanol, D-glucose, bovine serum albumin (Merck Millipore, Darmstadt, Germany), glacial acetic acid, heptanesulfonic acid, methanol, glutathione, NaOH, EDTA, dimethyl sulfoxide, L-DOPA, dopamine hydrochloride, S-(−)-raclopride (+)-tartrate salt, R-(−)-deprenyl hydrochloride, pargyline hydrochloride, ascorbic acid, (S)-(−)-sulpiride (Tocris, Bristol, United Kingdom), (−)-quinpriole Hydrochloride (Tocris), *R*-22[30] (gift of Dr. Amy Newman, synthesized at NIDA, NIH, Baltimore, MD), ML321[31] (synthesized at NINDS, NIH, Bethesda, MD) and [^{3}H]L-DOPA (Dihydroxyphenylalanine, L-3,4-[ring 2,5,6-^{3}H]) (American Radiolabeled Chemicals, St. Louis, MO).

Animal Husbandry

All animals were housed and handled in accordance with all appropriate NIH guidelines through the Columbia University Institute of Comparative Medicine, which approved the study. We abided by all appropriate animal care guidelines including ARRIVE guidelines for reporting animal research. Mice were housed in cages with a 12:12 light:dark cycle and had access to food and water *ad lib* at all times unless indicated otherwise. All efforts were made to ameliorate animal suffering.

Generation and breeding of transgenic D2R and D3R knockout mice

β-cell-specific D2R KO mice were generated by crossing homozygous RIP1-cre^{Herr} mice[32] (gift of Dr. Lori Sussel, Columbia University) that express Cre recombinase specifically in β-cells under the transcriptional control of the *Ins2* promoter with Drd2$^{loxP/loxP}$ mice[33] that carry two targeted loxP sites flanking *DRD2* exon 2 [gift of Dr. Marcelo Rubinstein (INGEBI) and Dr. Veronica Alvarez (NIH)]. Both parental transgenic strains were backcrossed with wildtype C57BL/6J mice for ≥10 generations to ensure an isogenic background in the tested progeny. Generation of global D3R KO mice is described in detail in our earlier studies[34].

Cell Culture and Pancreatic Islet Preparation

INS-1E cells (gift of Dr. Pierre Maechler, Université de Genève) were maintained in a humidified 37°C incubator with 5% CO_2. The cells were cultured with RPMI 1640 medium (Life Technologies Corp., Norwalk, CT) supplemented with 5% (v/v) heat inactivated fetal bovine serum, 2 mM glutamate, 10 mM HEPES, 1 mM sodium pyruvate, 100 units/mL penicillin, 100 μg/mL streptomycin, and 50 μM 2-mercaptoethanol. Cells used in the assays were tested and found to be negative for potential mycoplasma contamination. For mouse

pancreatic islet preparations, islets were obtained from 8–10 week-old male and female mice with either wildtype C57BL/6J, global D3R KO or β-cell-selective D2R KO genotypes. Pancreatic islets were freshly isolated via collagenase digestion of pancreata as described previously[35] and cultured free-floating overnight in RPMI 1640 media supplemented with 10% newborn calf serum, 100 units/mL penicillin, and 100 μg/mL streptomycin for use the following day. For insulin or DA secretion assays, islets were plated at 5–10 islets per well into 24-well plates. Each experiment used 2–3 mice to obtain sufficient numbers of islets where every condition was performed with n≥5 replicates.

Gene Expression Analyses

Pancreata, hypothalamus, and striatum from homozygous β-cell-selective D2R KO mice and littermate wildtype controls were rapidly dissected in cold PBS and placed into TRIzol Reagent (Life Technologies Corp., Carlsbad, CA). INS-1E cells were similarly placed into TRizol. Total RNA was isolated via the RNeasy Universal Plus Mini Kit (QIAGEN, Valencia, CA) according to the manufacturer's protocol. 500 ng of isolated mRNA from each tissue was reverse transcribed with random hexamers using the First Strand Transcription Kit (Roche, Basel, Switzerland). For qPCR assays, expression levels of L-Type Amino Acid Transporter 1 (*LAT1*), L-Type Amino Acid Transporter 2 (*LAT2*) and *Drd2* were detected using the QuantiTect SYBR Green PCR Kit (QIAGEN) and LightCycler 480 SYBRGreen I Master (Roche Diagnostics Corp., Indianapolis, IN) systems and quantified according to the $2^{\Delta\Delta Ct}$ method[36]. PCR products were confirmed in 1.5% agarose gels. Each assay was run in triplicate and independently repeated ≥3 times to verify the results. Levels of expression for *LAT1, LAT2* and *Drd2* were subsequently normalized to expression of *Rplp0* which encodes a ubiquitous ribosomal protein.

Primer design.—We used commercially available primers to assay *Drd2* gene expression (Quantitech #QT01169063, QIAGEN); primers for *Rplp0, LAT1*, and *LAT2* were designed using the Universal Probe Library Assay Design software package (Roche): *Rplp0*, forward 5′- GAGACTGAGTACACCTTCCCAC-3′, reverse 5′-ATGCAGATGGATCAGCCAGG-3′; *LAT1*, forward 5′-TCTTCGCCACCTACTTGCTC-3′, reverse 5′-GCCTTTACGCTGTAGCAGTTC-3′; *LAT2*, forward 5′-CTGGCTGCCATCTGTTTGT-3′, reverse 5′-TCTGCACAATACCCATGATGA-3′. Analysis of melting curves confirmed primer specificity.

Dopamine Secretion Assay

DA secretion assay.—For the cell-based DA secretion assay, INS-1E cells were seeded into a 24-well plate at an initial seeding density of 5.0×10^5 cells/well. Mutant and wildtype pancreatic islets were also seeded into a 24-well plate at a density of 5 islets/well and cultured free-floating overnight in RPMI 1640 media supplemented with 10% fetal bovine serum. On the experimental day, cells or islets were glucose-starved (1 h, 37°C) in KRB buffer (132.2 mM NaCl, 3.6 mM KCl, 5mM $NaHCO_3$, 0.5 mM NaH_2PO_4, 0.5 mM $MgCl_2$, 1.5 mM $CaCl_2$, and 0.001 g/mL bovine serum albumin). 30 μM L-DOPA was added 30 min prior to 20 mM glucose stimulation (90 min, 37°C). We chose the 30 μM L-DOPA concentration for use in this assay on the basis of its ability to generate sufficient detectable levels of DA and associated metabolites in our HPLC assay, and because this concentration

is below its IC_{50} for effects on GSIS (see Figure 3). At assay conclusion, supernatants and/or cell lysates were collected from each sample. For assays relying on DA detection from cell lysates, a monoamine oxidase inhibitor cocktail (10 μM deprenyl, 10 μM pargyline) was added 15 min following the initiation of the starvation period. Cell lysates were prepared by removing adherent cells with Enzyme-Free Cell Dissociation Solution (EMD Millipore; 5 min, 37°C) followed by sonication (Bioruptor, Cosmo Bio USA, Carlsbad, CA). Monoamine content was protected from oxidation by addition of cold HeGa solution (0.1 M glacial acetic acid, 0.1 mM EDTA, and 0.12% oxidized L-glutathione, pH 3.7) and immediately placed on ice.

Measurement of DA by HPLC.—Cell supernatants and lysates were syringe-filtered (0.20 μm filter; Thermo Scientific, Somerset, NJ) and analyzed via High Performance Liquid Chromatography with electrochemical detection (HPLC-EC), as previously described[37]. Briefly, samples were separated on a C18 reverse-phase column (VeloSep RP-18 Cartridge Column; Perkin Elmer, Waltham, MA) with the mobile phase consisting of 45 mM KH_2PO_4·H2O, 0.2 mM EDTA, 1.4 mM heptanesulfonic acid and 5% methanol, pH 3.5. DA and its derivatives were detected on an ESA Coulochem II electrochemical detector (Thermo Scientific) at 300 mV oxidation potential. The IGOR Pro software package (WaveMetrics, version 6, Lake Oswego, OR) quantified DA for each sample from areas under the HPLC peaks based on defined calibration curves.

[^{3}H]L-DOPA Uptake Assay

INS-1E cells were seeded into a 24-well plate at an initial density of 5.0×10^5 cells/well. RPMI 1640 media was exchanged 24 h after seeding and experiments were conducted the following day. On the experimental day, cells were first glucose-starved in KRB (1 h, 37°C). Uptake of [^{3}H]L-DOPA was initiated by addition of 2 μM [^{3}H]L-DOPA (specific radioactivity of 3 Ci/mmol) for all treatment conditions. Reactions were stopped by aspirating [^{3}H]L-DOPA-containing buffer and cells were washed two times with KRB. Cells were solubilized with 5% SDS, mixed with scintillation cocktail and the samples were counted in a Packard Tri-Carb 2100 TR liquid scintillation analyzer (PerkinElmer, Hopkinton, MA). Known amounts of [^{3}H]L-DOPA were used as a standard to transform cpm into pmol.

Insulin Secretion Assay and Measurement

In vitro insulin secretion assay.—A detailed account of insulin measurement via homogenous time resolved fluorescence (HTRF) was described earlier[38, 39]. Briefly, INS-1E cells were seeded into a 24-well plate at an initial seeding density of 5.0×10^5 cells/well. RPMI 1640 media was exchanged 24 h after seeding and experiments conducted the following day. On the experimental day, cells were glucose-starved (1 h, 37°C) in KRB and subsequently stimulated with 20 mM glucose (90 min, 37°C). For the mouse islet secretion assay, islets were seeded in 24-well plates and glucose-starved in KRB (1 h, 37°C). Islets were then stimulated with 20 mM glucose ± additional drugs followed by supernatant collection. Insulin content for each sample was measured using an HTRF-based assay (Cisbio Bioassays, Codelet, France) as described earlier[39]. Fluorescence emissions were read by a multi-mode microplate reader (PHERAstar FS, BMG Labtech, Ortenberg,

Germany). In drug competition assays, INS-1E cells were first pre-incubated with 100 μM L-DOPA (in KRB; 30 min, 37°C) during glucose starvation followed by drug addition in the continued presence of L-DOPA. We chose the 100 μM L-DOPA concentration on the basis of its ability to inhibit GSIS at close to maximal levels according to its dose-response curve (see Figure 3). Individual concentrations of the D2R and D3R receptor blockers were chosen on the basis of their respective EC_{50} values from drug competition assay inhibitor dose-response curves (data not shown). We used GraphPad Prism software (version 6.0, GraphPad Software, Inc., La Jolla, CA) to interpolate raw HTRF values from the experimental samples to known insulin concentration values to derive the final insulin concentrations.

In vivo insulin secretion.—Baseline serum insulin measurements were collected from homozygous β-cell-selective D2R KO mice and wildtype littermate controls immediately following an overnight fast (12–16 h). After the fast, each mouse was administered a single food pellet over a 15–20 min feeding period. Serum was collected 20 min thereafter for measurement of postprandial insulin levels. To control for inter-subject variability, postprandial serum insulin values were normalized to the respective pre-meal fasting serum insulin levels of each mouse. This postprandial/fasting serum insulin ratio was employed as a measure of postprandial elevation of insulin relative to the pre-meal fast. Serum insulin was measured by ELISA (ALPCO, Salem, NH). Absorbance measurements for the samples were made using a Biotek Synergy 2 microplate reader (BioTek Instruments, Inc., Winooski, VT). Potential values >3 standard deviations from the mean were excluded. All samples were randomized using numbered codes and analyzed in a double-blind manner.

Glucose measurement.—In parallel to the insulin measurements, corresponding glucose measurements under fasting and postprandial conditions were assayed. For each condition, glucose was measured from the same blood collected for the insulin measurements from each mouse via the OneTouch Ultra glucometer (LifeScan, Inc., Inverness, Scotland). All samples were randomized using numbered codes and analyzed in a double-blinded manner.

Glucose Tolerance Testing.—Intraperitoneal (i.p.) glucose tolerance tests (ipGTTs) were performed as described previously[40]. Briefly, after a 5 h fast, mice were injected intraperitoneally with glucose (2 g/kg body weight) and blood glucose levels were determined from tail vein samples at 0, 15, 30, 60 and 120 minutes after the injection. All samples were randomized using numbered codes and analyzed in a double-blinded manner.

Index of insulin sensitivity.—Homeostasis model assessment of insulin resistance (HOMA- IR) was calculated as (fasting glucose level × fasting insulin level)/22.5 as described previously[41, 42].

Statistical Analyses

SPSS (version 18.0, IBM, Armonk, NY) was used for all statistical analyses. Drug dose response curves were fit via non-linear regression of Log (ligand) versus normalized % maximal insulin secretion values. EC_{50} and IC_{50} values were computed via a nonlinear, least-squares regression analysis using GraphPad Prism (version 7.0). We used univariate ANOVA (α=0.05) followed by Dunnett post-hoc t-tests to compare between-group

differences using SPSS; Bonferroni post-hoc t-tests were conducted for multiple comparisons between effects of drug treatment on insulin secretion. We used repeated measures 2-way ANOVA to compare between-group differences in our intraperitoneal glucose tolerance tests. 2-tailed t-tests were used to analyze *in vivo* insulin secretion data and DA secretion results, as well as for comparison of insulin sensitivity indices across different groups. Variance was similar between the groups being statistically compared. 13Sample size was initially chosen on the basis of power analyses assuming an effect size of 0.60, power level of 0.80, and a probability level for statistical significance of 0.05 and was calculated via the G*Power software package (University of Düsseldorf, Germany).

Results

Glucose-stimulated DA release requires DA precursor L-DOPA

There is increasing evidence that insulin-secreting β-cells are an important site of non-neuronal DA synthesis and utilization[12, 17]. However, the mechanisms by which these cells synthesize, store and release DA, particularly during states of stimulation, remain poorly understood. Therefore, we first examined the capacity of pancreatic β-cells to secrete endogenously stored DA during GSIS using the INS-1E cell system (Figure 1). Surprisingly, we found no detectable DA or its metabolites, including homovanillic acid (HVA) and 3,4-dihydroxyphenylacetic acid (DOPAC), secreted from the cells during high glucose stimulation by HPLC analysis (Figure 1a); we observed similar results in mouse pancreatic islets (Figure S1a). To determine whether our stimulation conditions were insufficient to promote DA release from putative intracellular DA stores, we analyzed cellular DA content. Lysates of INS-1E cells contained negligible amounts of intracellular DA (Figure S1b, black bar); mouse islet lysates similarly did not contain detectable intracellular DA (data not shown). Our data suggest that despite the presence of DA biosynthetic machinery, in the absence of an exogenous source of DA or its precursors, INS-1E cells and islets do not accumulate significant intracellular DA stores.

Since β-cells express DA biosynthetic enzymes including AADC[25], we hypothesized that: (1) these cells are capable of synthesizing *de novo* stores of cellular DA by converting DA precursors such as L-DOPA into DA, and (2) that this newly synthesized DA could be subsequently released in response to stimulation. Indeed, pre-incubation with L-DOPA produced a robust DA signal in the secreted supernatant during high glucose stimulation of INS-1E cells (Figure 1b) or mouse islets (Figure S1a). Furthermore, high glucose stimulation enhanced secretion of the newly synthesized DA by 70% relative to the unstimulated control (P=0.013; Figure 1c). As above, in the absence of L-DOPA pre-treatment, there was no detectable secreted DA in either the basal or glucose-stimulated conditions (Figure 1c). Our results therefore suggest that β-cells have the capacity to produce and secrete DA when provided DA precursors and that this release is regulated by stimulation with high glucose. These findings are analogous to the ability of β-cells to rapidly mobilize and secrete insulin in response to stimulation[43, 44]..

We investigated the possibility that the relative absence of intracellular DA in β-cells was due to rapid DA degradation via the cellular catabolic machinery. Prior work demonstrated that β-cells express both MAOA and MAOB[26, 45], which we functionally confirmed by

observing 3,4-dihydroxyphenylacetic acid (DOPAC), the product of MAO metabolism of DA, following L-DOPA pre-treatment (Figures 1b, S1a). Inhibition of β-cell MAO activity during L-DOPA pre-treatment using the monoamine oxidase inhibitors (MAOIs) deprenyl (MAOB inhibitor) and pargyline (MAOA/B inhibitor) led to a 30-fold increase in intracellular DA levels compared to non-MAOI treated cells (P=0.009; Figure S1b). These data suggest that MAO activity represents an important source of intracellular DA degradation. Therefore, we measured the kinetics of DA biosynthesis in the presence of MAOIs to avoid potential confounds attributable to concomitant MAO-mediated catabolism. Addition of L-DOPA to INS-1E cells revealed the rapid appearance of intracellular DA prior to the onset of glucose stimulation (period from −30 min to 0 min; Figure S1c). However, within 30 min of stimulation, only 50% of the newly synthesized intracellular DA remained within the cells relative to the peak DA levels evident at the start of stimulation (0 min). These data suggest that a significant fraction of *de novo* synthesized cellular DA is released, particularly during stimulation (Figure S1c).

DA release is enhanced by glucose stimulation due to increased L-DOPA uptake

We hypothesized that enhanced β-cell DA secretion in response to glucose stimulation (Figure 1c) was due to increased L-DOPA uptake and subsequent DA synthesis, which generates an increased pool of releasable DA. To test this, we first characterized the machinery responsible for β-cell L-DOPA uptake.

In the central nervous system (CNS), intestines and kidneys, L-DOPA is a substrate for L-type amino acid transporters (LATs), which are instrumental in cellular L-DOPA uptake[46–48]. We analyzed expression of LAT1 and LAT2 isoforms by qPCR in INS-1E cells and wildtype mouse pancreatic islets and compared this to levels in the mouse hypothalamus and striatum – two brain regions associated with dopaminergic neurotransmission[49, 50]. LAT1 was transcribed to comparable levels in INS-1E cells and islets compared to hypothalamus and striatum (P>0.05; Figure 2a). LAT2 was also present in INS-1E cells, islets and the examined brain regions but was transcribed at higher levels in INS-1E cells relative to islets or striatum and hypothalamus (P=0.006; Figure 2b). To examine the functional role of LATs in β-cell L-DOPA uptake, we used a [^{3}H]L-DOPA tracer to measure the intracellular accumulation of L-DOPA in INS-1E cells under unstimulated and glucose-stimulated conditions. As a control, unlabeled L-DOPA substrate was used to define nonspecific accumulation of tracer (Figure S2). Treatment with the LAT1/LAT2 competitive substrate, 2-aminobicyclo-(2,2,1)-heptane-2-carboxylic acid (BCH), also inhibited [^{3}H]L-DOPA accumulation (Figure S2, green bars). Additionally, triiodothyronine (T_3), a competitive LAT1-specific blocker that does not act on LAT2[51], inhibited [^{3}H]L-DOPA uptake by 70% (Figure S2, blue bar). Thus, LAT1 likely is responsible for most of L-DOPA transport, with a smaller but significant contribution by LAT2.

We next examined the kinetics of L-DOPA uptake during glucose stimulation using [^{3}H]L-DOPA to monitor intracellular accumulation of L-DOPA (Figure 2c). [^{3}H]L-DOPA uptake almost doubled within 30 min of glucose stimulation relative to the unstimulated control (1.7-fold increase, P=0.0005; Figure 2c). Total DA uptake over the entire 120 min experiment was increased 2.5-fold compared to the control (P=0.002; Figures 2c, d). We

also observed a progressive decrease in accumulated intracellular [^{3}H]L-DOPA over time (Figure 2c). We investigated whether this decrease in tracer signal was due to conversion of [^{3}H]L-DOPA to [^{3}H]DA, which could then be released out of the cell. Therefore, we treated cells with 5 μM benserazide, a potent inhibitor of aromatic acid decarboxylase (AADC), to block conversion of L-DOPA to DA[52]. Benserazide treatment significantly attenuated the decrease in accumulated intracellular [^{3}H]L-DOPA we observed during glucose stimulation, with 2-fold more intracellular [^{3}H]L-DOPA remaining at the study conclusion relative to the benserazide-untreated control (P=0.001; Figures 2c, d). Overall, our data demonstrate that glucose stimulation primes *de novo* DA biosynthesis in β-cells by enhancing DA precursor uptake followed by AADC-dependent conversion to DA, which can be released to initiate signaling at DA receptors in the plasma membrane.

D2R and D3R signaling modulates glucose-stimulated insulin secretion

Given that L-DOPA uptake and DA release are coupled to glucose stimulation, we next investigated dopaminergic signaling at the receptor level during GSIS. Using our recently developed HTRF-based assay for rapid measurement of insulin secretion[39], we first examined the effects of pre-loading L-DOPA on GSIS in INS-1E cells. Increasing L-DOPA concentrations inhibited GSIS in a dose-dependent manner (IC_{50}=38.3 μM; Figure 3a). Pre-treatment of cells with AADC blocker benserazide abolished the inhibitory effects of L-DOPA on GSIS (Figure 3a), implicating DA, and not a direct action of L-DOPA, in the inhibition of GSIS. These data are consistent with growing evidence suggesting that DA is a negative regulator of insulin secretion[11, 17, 39].

We examined whether DA D_2-like receptors were responsible for GSIS inhibition following L-DOPA treatment. Quinpirole, an agonist of both D2R and D3R[53], dose-dependently inhibited GSIS (IC_{50}=10.3 μM; Figure 3b). Conversely, the D2R/D3R blocker raclopride blocked L-DOPA's inhibitory effects on GSIS in a dose-dependent manner, returning the cells to near-maximal levels of insulin secretion (EC_{50}=1.2 μM; Figure 3c). We confirmed these findings with the APD sulpiride, another D2R/D3R-selective blocker[54], which similarly attenuated L-DOPA's inhibitory effects on GSIS (EC_{50}=1.5 μM; Figure S3a). Importantly, sulpiride has been shown to be membrane-impermeant at relevant pharmacological concentrations[55]. Thus, its ability to effectively block the inhibitory effect of L-DOPA on GSIS is consistent with an extracellular action of DA on plasma membrane D2R/D3R and not with intracellular signaling. Since most pharmacological tools have limited receptor selectivity amongst the different DA D_2-like receptor subtypes[18], it has remained unclear which of these receptors is responsible for mediating DA's inhibition of GSIS. To determine the relative contributions of D2R and D3R in mediating GSIS, we used recently developed D2R-selective and D3R-selective compounds to block the respective activities of these two receptors. We observed that as little as 300 nM of the D3R-selective blocker R22[30] successfully reduced L-DOPA's inhibition of GSIS (EC_{50}=136 nM; P<0.0001), albeit to a lesser degree than raclopride or sulpiride, which block both D2R and D3R. Likewise, the D2R-selective inhibitor ML321[31] (3 μM) also partially reduced L-DOPA-induced GSIS inhibition (EC_{50}=1.2 μM, P<0.0001; Figure S3b). Taken together, these data suggest that both D2R and D3R mediate GSIS inhibition, and that greater inhibition is achieved through joint receptor action.

D2R and D3R knockout attenuates L-DOPA's inhibitory modulation of GSIS

To complement our findings with the D2R- and D3R-selective drugs, and to establish that our findings in the INS-1E cells are consistent with those in a more native preparation, we used a parallel genetic strategy by examining the effects of D2R or D3R deletion on GSIS in pancreatic islets. Wildtype C57BL/6J (WT) mice exhibited a significant dose-dependent decrease in GSIS following L-DOPA treatment (10 μM: P=0.006; 30 μM: P<0.0001) compared to the high glucose alone control (Figure 4a). In contrast, L-DOPA's GSIS inhibition was abolished in pancreatic islets from global D3R KO mice treated with 10 μM or 30 μM L-DOPA (P>0.05; Figure 4b). To probe D2R's role in GSIS inhibition, we generated the first β-cell-specific D2R KO mouse. We validated the tissue specificity of D2R knockdown by comparing D2R expression in brain and pancreas via qPCR. D2R expression was significantly reduced by 91% in pancreatic islets of β-cell-specific D2R KO mice relative to WT littermate controls (P=0.023; Figure S4). In contrast, there was no significant difference in D2R expression in hypothalamus or striatum, regions of known D2R expression[29, 56], in KO mice compared to the controls (P>0.05; Figure S4). Using islets from these β-cell-specific D2R KO mice, we observed that GSIS inhibition by L-DOPA was absent at 10 μM (P>0.05) and largely attenuated at 30 μM (P=0.05; Figure 4c). Overall, our data were consistent with the pharmacological data suggesting a joint role for both D2R and D3R in mediating L-DOPA's inhibition of GSIS.

We also examined the specific, respective contributions of D2R and D3R signaling to modulation of GSIS independently of islet DA biosynthesis following L-DOPA treatment by directly treated WT, D2R KO and D3R KO mouse pancreatic islets with increasing concentrations of exogenous DA (Figures 4d-f). WT islets exhibited significant dose-dependent GSIS inhibition across the range of DA concentrations tested (100 nM-10 μM, P<0.001; Figure 4d). Islets from β-cell-specific D2R KO or global D3R KO mice were less sensitive to DA's inhibitory effects on GSIS. While there was no significant GSIS inhibition following treatment with the lowest DA concentration in D2R or D3R KO islets (100 nM, P>0.05; Figures 4e, f), both D2R KO and D3R KO islets exhibited significant GSIS inhibition at higher DA concentrations (Figure 4e, f), consistent with a role for both receptors.

Glucose-stimulated DA secretion is reduced in D2R and D3R KO islets

Direct applications of high DA concentrations effectively inhibited GSIS in both D2R and D3R KO islets. This suggests that the residual D2R receptors in D3R KO islets and residual D2R receptors in D3R KO islets were capable of mediating DA's inhibitory effects on GSIS. This contrasts with the dramatic impairment of L-DOPA-mediated inhibition of GSIS in the D2R and D3R KO islets (Figures 4b, c). Although it was possible that the DA produced from L-DOPA supplied in these experiments was insufficient to produce adequate GSIS inhibition, we considered the possibility that the respective KO islets may have impaired DA synthesis and/or release in response to L-DOPA pre-treatment. To test this, we compared the capacity of WT and respective KO islets to secrete *de novo*-synthesized DA during glucose stimulation using pancreatic islets pre-treated with L-DOPA from global D3R KO and β-cell-specific D2R KO mice versus WT littermate controls (Figure S5). We found that D3R KO islets secreted significantly less DA during glucose stimulation (32% reduction;

P=0.012) relative to the WT littermate controls (Figure S5a). Similarly, D2R KO islets secreted 55% less DA compared to WT (*P*<0.0001; Figure S5b). These findings explain the greater impairment of L-DOPA-mediated GSIS relative to the direct actions of DA in the KO islets, and raise important mechanistic questions for future investigation.

D2R KO in β-cells disrupts postprandial insulin regulation *in vivo*

We investigated D2R's role in maintaining insulin homeostasis *in vivo* using our β-cell-selective D2R KO mice. We measured the effects of D2R KO on changes in serum insulin levels in response to a meal challenge. While there were no significant differences in fasting serum insulin levels between D2R KO and the WT control mice preceding the meal challenge (*P*>0.05; data not shown), we observed significantly higher serum insulin levels in D2R KO mice following a meal challenge (*P*=0.038; Figure 5a). We explored the possibilities that these insulin increases were in response to concomitant elevations in blood glucose and/or increased insulin resistance in the D2R KO mice relative to the WT control animals. Comparisons of fasting or postprandial glucose levels between the two genotypes did not reveal any significant differences (*P*>0.05; Figure 5b). Furthermore, we found no significant differences in insulin sensitivity either at basal or post-glucose infusion timepoints between D2R KO and WT mice as measured by intraperitoneal glucose tolerance testing (ipGTT) (*P*>0.05; Figure 5c) or via calculation of the homeostasis model assessment of insulin resistance (HOMA-IR)[42] (*P*>0.05; WT: 4.3±0.8, D2R KO: 8.9±2.4). These data suggest that the constituents of the food pellets provided in the oral challenge (see Methods) were sufficient to generate DA precursors that are absent when glucose is administered i.p. Importantly, our results also suggest that the differences in postprandial insulin levels may therefore be a consequence of direct changes in insulin secretion rather than in response to insulin resistance or elevated blood glucose levels in the D2R KO mice. Overall, these data suggest that D2R modulation of insulin release is especially sensitive to acute food intake. Moreover, blunted D2R signaling in β-cells may cause decreased DA-mediated GSIS inhibition and lead to the postprandial hyperinsulinemic state observed.

Discussion

Though DA signaling has long been studied in the CNS, there is increasing evidence that it also plays key physiological roles in the periphery[3, 17, 22, 57]. While the sympathetic nervous system was originally implicated as an important regulator of blood pressure by DA[58], the intrarenal DA system also plays a critical role in modulation of both blood pressure and salt/water balance independently of neural DA input[59]. Renal proximal tubule cells express the DA biosynthetic machinery as well as DA D_2-like receptors including D2R[57, 60, 61]. Uptake of circulating L-DOPA fuels local DA biosynthesis and release by these cells followed by autocrine/paracrine DA signaling at renal DA receptors to maintain fluid and electrolyte homeostasis and normal blood pressure[59, 61–63]. There is increasing awareness that these findings are not restricted to the kidneys and are found in other tissues and organ systems as well. Pancreatic β-cells similarly express a dopaminergic system[17]. In addition to DA's emerging involvement in the regulation of calcium flux, cell proliferation and survival in β-cells[12, 27], earlier work suggested that the β-cell dopaminergic system can play important

roles in metabolism through DA's function as a negative modulator of insulin secretion[3, 10, 17, 38].

Rodent and human pancreatic β-cells were previously shown to possess the machinery for DA biosynthesis including TH and AADC[11, 12, 64]. Yet, despite expression of these DA biosynthetic enzymes, our data shows negligible intracellular DA stores in INS-1E cells and mouse pancreatic islets, consistent with earlier studies in rodent islets[12, 64]. Nevertheless, both TH expression and *de novo* DA synthesis are evident in human and rodent islets, suggesting that DA synthesis and signaling are physiologically relevant[64]. Evidence however suggests that levels of *de novo* DA biosynthesis are highly variable across species, and even within a species, there are wide disparities in TH expression and/or activity[64]. Moreover, *in vivo* TH activity is sensitive to acute dietary manipulations, further complicating accurate estimations of intracellular DA stores both at rest and during periods of cell stimulation[65]. Recent evidence demonstrates that TH expression is crucial for normal development of β-cells, with TH-synthesized DA acting as a pro-β-cell stimulus[66]. Thus, continued TH expression in adult β-cells may be a remnant of its developmental relevance. Overall, our results builds upon earlier work suggesting that steady state levels of intracellular DA are ordinarily maintained at very low levels but can be significantly increased when DA precursors such as L-DOPA are made available to β-cells[67].

Given the importance of acute L-DOPA uptake for β-cell DA synthesis and secretion, we further characterized the transporters responsible for L-DOPA uptake into β-cells. Besides cell uptake of branched-chain amino acids, System-L amino acid transporters (LATs) are also high-affinity transporters of L-DOPA[68]. Recent studies suggest that LAT activity mediates β-cell insulin secretion, although the precise identities of the transporters and the mechanisms have remained unclear[68]. We recently showed that LAT1 is expressed in human and rodent pancreatic islets as well as in INS-1E cells[11, 68]. Here we demonstrated for the first time that INS-1E cells and mouse pancreatic islets also express an additional LAT isoform, LAT2, at levels comparable to dopaminergic brain regions including striatum and hypothalamus. Functionally, our results suggest that while LAT1 transporter activity contributes significantly to L-DOPA uptake into β-cells, LAT1 likely works in concert with LAT2 to ensure efficient L-DOPA uptake. These results are consistent with previous work showing that LAT2 is important in postprandial transport of L-DOPA in intestinal epithelial cells[48].

Significantly, glucose stimulation markedly enhanced L-DOPA uptake in INS-1E cells. These results demonstrate that stimulatory conditions that classically culminate in insulin secretion (*e.g.* cell depolarization) also potentiate DA precursor uptake and increase DA secretion. Our findings are consistent with studies examining L-DOPA uptake in renal proximal tubule cells that similarly demonstrated enhanced L-DOPA uptake in response to cell stimulation[69]. Insulin stimulation of the renal cells triggered a cascade of Akt and protein kinase C ζ-dependent signaling that resulted in increased cellular L-DOPA uptake. Overall, we find a system where β-cells can tune the amount of DA precursor uptake, synthesis and secretion in response to cell activity. These results raise the question: what are sources of this L-DOPA?

L-DOPA is present in considerable amounts in the GI tract, supplied in large part by dietary sources[70–72]. This L-DOPA contributes significantly to DA synthesis in non-neuronal cells in the periphery[73]. The newly synthesized DA is sulfoconjugated to create DA sulfate and distributed throughout the periphery[73]. Indeed, following meal ingestion, plasma DA sulfate levels increase significantly in humans (>50-fold) as well as in rodents[70–74]; mixed meals of protein and carbohydrates are especially implicated in this rise in postprandial DA[17, 27]. As sympathectomy does not affect postprandial increases in L-DOPA, it is unlikely that endogenously-produced catecholamines from local sympathetic innervation contribute to this phenomenon[71, 74]. Importantly, feeding studies in rodents and humans showed that the postprandial appearance of L-DOPA and DA in the circulation is within 60 min of feeding[70, 73] which is within the overall range of our experiments.

We further dissected the respective contributions of D_2-like receptors D2R and D3R to dopaminergic inhibition of GSIS. Earlier pharmacological studies suggested that drug actions on D3R alone modified GSIS, while other work used drugs acting on both receptors; to date, no clear consensus exists regarding whether one or both receptors are necessary to modulate insulin secretion[10–12]. The structural and functional similarities between D2R and D3R[75] make it difficult for most existing pharmacological tools to accurately discriminate between the two receptors[76, 77]. However, using recently developed pharmacological agents with significantly improved selectivity for either D2R or D3R, we found that D2R-selective blocker ML321 (>50-fold selectivity for D2R over D3R)[18, 31] or D3R-selective inhibitor R22 (>100-fold selectivity for D3R over D2R)[30, 77] only partially attenuated L-DOPA's inhibition of GSIS. In contrast, drugs that targeted both D2R and D3R (*e.g.* sulpiride and raclopride) blocked L-DOPA's inhibitory effects on GSIS almost completely. Likewise, treatment with the D2R/D3R agonist quinpirole produced dose-dependent GSIS inhibition with a potency comparable to that of DA. Our data therefore suggest that D2R and D3R function together to modulate dopaminergic inhibition of GSIS. Previous work employing different D2R- and D3R-selective antagonists implicated only D3R in regulation of GSIS[12]. Such discrepancies may be attributed to potential differences in receptor selectivity of the D2R- and D3R-selective drugs tested and/or off-target effects for each of these agents.

In parallel with our pharmacological approaches, we used a genetic strategy to selectively knock out D2R expression in β-cells. Earlier work examining preexisting global D2R KO mouse models demonstrated impaired overall glucose homeostasis[22]. However, these efforts were complicated by complex neuroendocrine and metabolic phenotypes, including hyperprolactinemia and dwarfism due to D2R's important roles in the CNS. This has made it difficult to determine specific CNS versus peripheral contributions of D2R on metabolic regulation[13, 19, 22]. To address this, we have created the first β-cell-specific D2R KO mouse to focus on D2R's specific potential roles in modulating GSIS in pancreatic β-cells. In parallel, we used islets from a global D3R mouse to similarly probe D3R's roles in GSIS. While D3R KO attenuated L-DOPA's inhibitory effects at all L-DOPA concentrations, islets from the β-cell-specific D2R KO islets were still sensitive to GSIS inhibition at the higher 30 μM L-DOPA concentration. It remains possible that the D3R still expressed in D2R KO islets may continue to signal and thus contribute to the residual L-DOPA inhibition. In contrast, continued D2R expression in D3R KO islets may be insufficient to produce the DA

signaling necessary to significantly diminish GSIS, especially since D2R has a lower DA affinity compared to D3R[77].

In contrast to L-DOPA treatment, DA-induced GSIS inhibition in either D2R or D3R KO islets was decreased, though still intact at high DA concentrations. We infer that this GSIS inhibition is likely due to dopaminergic signaling at the remaining D_2-like receptors. Here we show that D_2-like receptors also regulate levels of secreted DA in β-cells. With less DA being released from D2R KO or D3R KO islets following L-DOPA pre-treatment, DA-mediated inhibition of GSIS was blunted. This would be consistent with a role for these receptors in promoting DA synthesis, vesicular loading and/or trafficking or efficiency of DA release. Curiously, this is not consistent with the inhibition of DA synthesis and release mediated by D2R autoreceptors in the CNS[49, 78]. Further work is needed to explore the signaling mechanisms responsible for these divergent effects. Importantly, at the receptor level, exogenous DA application still lead to significant GSIS inhibition, indicating that the remaining D_2-like receptors still function in the respective KO islets.

In examining the metabolic sequelae of β-cell-selective D2R knockdown *in vivo*, we found a substantially greater (3-fold) increase in postprandial insulin response compared to WT littermate controls. Given the absence of significant derangements in basal and postprandial glucose levels or diminished insulin sensitivity, our results suggest that the heightened postprandial insulin response in D2R KO mice was most likely attributable directly to changes in insulin secretion. Importantly, our data further underscore the critical relationship between food intake and dopaminergic regulation of insulin secretion given that this D2R-mediated insulin response was unmasked in response to feeding. Nevertheless, future studies are needed to further characterize this phenomenon including more direct assessments of β-cell secretory function in response to food challenges.

Since uptake of dietary L-DOPA is a key avenue for stimulating DA production in β-cells[27, 67, 72, 73], we propose that: (1) in response to food intake, there is an increase in circulating L-DOPA in the GI circulation supplying pancreatic β-cells; (2) L-DOPA uptake through LAT1 and LAT2 boosts β-cell DA stores. (3) As postprandial blood glucose levels rise, the β-cells depolarize, releasing both insulin and DA; (4) the released DA binds to D2R and D3R, which work together to inhibit further GSIS. Our model therefore suggests that β-cells can tune the extent of dopaminergic inhibition of GSIS on the basis of DA precursor availability, which is based on the size of the meal and metabolic load. Although it is likely that an ensemble of D_2-like receptors work together in β-cells to modulate GSIS, our findings suggest that disrupting signaling through one or more D_2-like receptors, as in the case of β-cell-selective D2R KO, is sufficient to produce metabolic disturbances *in vivo*. Furthermore, since APDs chronically block the D2R and D3R signaling mediating this circuit, our findings may provide an important new mechanism for the metabolic dysfunction induced by APDs.

We ultimately posit that the hyperinsulinemia and insulin resistance at the root of many of APDs' metabolic disruptions may therefore be caused by their actions at peripheral dopaminergic targets. Similarly, our results may explain longstanding findings demonstrating hyperglycemia in both rodents and in humans treated with L-DOPA[79].

Indeed, up to 50–80% of Parkinson's disease patients have abnormalities in glucose homeostasis, and L-DOPA treatment has been shown to cause or exacerbate hyperglycemia[80]. L-DOPA's inhibition of insulin secretion may contribute to the chronic hyperglycemia observed clinically[80] – an effect previously reported in rat models.[81]

Our results are consistent with findings from prior studies. Indeed, earlier work showed that acute D2R/D3R blockade with as little as a single dose of raclopride enhanced insulin secretion during hyperglycemic clamps of healthy rats[82]. Studies in healthy human subjects also demonstrated that acute treatment with a single dose of the APD amisulpride, a relatively selective D2R/D3R antagonist[83], was sufficient to stimulate increased β-cell insulin secretion[84]. Similarly, a 9-day administration of olanzapine in healthy human subjects led to elevations in postprandial insulin[85]. Chronically, such hyperinsulinemic states may contribute to desensitization of insulin-responsive tissues (*e.g.* liver, adipose tissue, skeletal muscle) to insulin and ultimately culminate in insulin resistance[3]. Moreover, it has been suggested that prolonged insulin secretion following D2R/D3R blockade by APDs may deplete β-cell insulin granule stores over time, further exacerbating drug-induced metabolic disturbances[82]. It is possible that the homeostatic mechanisms including redundant regulatory and counterregulatory systems could offset the impact of APD blockade[3, 86]. However, even with lifelong knockdown of D2R in the β-cells, we still see significant dysregulation of insulin secretion in adult animals, suggesting that the system has not sufficiently compensated. Nevertheless, there are likely other mechanisms that also contribute to the disruptions in glucose homeostasis or the development of tissue-level insulin resistance by APDs including insulin-independent mechanisms associated with cellular glucose uptake and transport[86, 87].

Overall, our work sheds light on fundamental mechanisms of DA signaling outside of the CNS and its implications for regulation of metabolism. These findings may also provide new insights into how disruption of pancreatic dopaminergic signaling can produce metabolic disturbances and opens the door to novel therapeutic approaches targeting peripheral DA receptors.

Supplementary Material

Refer to Web version on PubMed Central for supplementary material.

Acknowledgments

The authors would like to gratefully thank and acknowledge Drs. Domenico Accili, Rudolph Leibel, Amy Newman, Marcelo Rubinstein, Lori Sussel, Ruth Singer, Jacob Ballon, Michael McCarthy, Mark Sonders, Nicolas Pierre, Marília Gueiros, Thue Schwartz, Birgitte Holst, Andreas Madsen, Jeffrey Brodsky, and Ms. Emily George for helpful discussions, reagents and assistance throughout this work. This research was supported by a Department of Defense PRMRP Investigator Initiated Award PR141292 (Z.F.), NIDA K08 DA031241 award (Z.F.), Louis V. Gerstner, Jr., Scholars Program (Z.F.), Leon Levy Foundation (Z.F.), the John F. and Nancy A. Emmerling Fund of The Pittsburgh Foundation (Z.F.), NIDA F32 DA044696 (P.C.D.), NINDS R01 NS075222 (E.V.M.), NIMH R01 MH093672 (C.K.), NINDS Intramural Program (D.R.S., R.B.F.), NIDDK R01 DK116583 (P.E.H.), NARSAD Distinguished Investigator Award (J.A.J.), NIMH R01 MH54137 (J.A.J.), and NIMH T32 MH018870 (J.A.J.).

References

1. Fleischhacker WW, Siu CO, Boden R, Pappadopulos E, Karayal ON, Kahn RS et al. Metabolic risk factors in first-episode schizophrenia: baseline prevalence and course analysed from the European First-Episode Schizophrenia Trial. Int J Neuropsychopharmacol 2012: 1–9.
2. Fabrazzo M, Monteleone P, Prisco V, Perris F, Catapano F, Tortorella A et al. Olanzapine Is Faster than Haloperidol in Inducing Metabolic Abnormalities in Schizophrenic and Bipolar Patients. Neuropsychobiology 2015; 72(1): 29–36. [PubMed: 26337616]
3. Freyberg Z, Aslanoglou D, Shah R, Ballon JS. Intrinsic and Antipsychotic Drug-Induced Metabolic Dysfunction in Schizophrenia. Frontiers in neuroscience 2017; 11: 432. [PubMed: 28804444]
4. Rajkumar AP, Horsdal HT, Wimberley T, Cohen D, Mors O, Borglum AD et al. Endogenous and Antipsychotic-Related Risks for Diabetes Mellitus in Young People With Schizophrenia: A Danish Population-Based Cohort Study. Am J Psychiatry 2017; 174(7): 686–694. [PubMed: 28103712]
5. Karam CS, Ballon JS, Bivens NM, Freyberg Z, Girgis RR, Lizardi-Ortiz JE et al. Signaling pathways in schizophrenia: emerging targets and therapeutic strategies. Trends Pharmacol Sci 2010; 31(8): 381–390. [PubMed: 20579747]
6. Ballon JS, Pajvani U, Freyberg Z, Leibel RL, Lieberman JA. Molecular pathophysiology of metabolic effects of antipsychotic medications. Trends in endocrinology and metabolism: TEM 2014.
7. Kapur S, Zipursky R, Jones C, Remington G, Houle S. Relationship between dopamine D(2) occupancy, clinical response, and side effects: a double-blind PET study of first-episode schizophrenia. Am J Psychiatry 2000; 157(4): 514–520. [PubMed: 10739409]
8. Kern A, Albarran-Zeckler R, Walsh HE, Smith RG. Apo-ghrelin receptor forms heteromers with DRD2 in hypothalamic neurons and is essential for anorexigenic effects of DRD2 agonism. Neuron 2012; 73(2): 317–332. [PubMed: 22284186]
9. Suzuki M, Hurd YL, Sokoloff P, Schwartz JC, Sedvall G. D3 dopamine receptor mRNA is widely expressed in the human brain. Brain Res 1998; 779(1–2): 58–74. [PubMed: 9473588]
10. Rubi B, Ljubicic S, Pournourmohammadi S, Carobbio S, Armanet M, Bartley C et al. Dopamine D2-like receptors are expressed in pancreatic beta cells and mediate inhibition of insulin secretion. J Biol Chem 2005; 280(44): 36824–36832. [PubMed: 16129680]
11. Simpson N, Maffei A, Freeby M, Burroughs S, Freyberg Z, Javitch J et al. Dopamine-mediated autocrine inhibitory circuit regulating human insulin secretion in vitro. Mol Endocrinol 2012; 26(10): 1757–1772. [PubMed: 22915827]
12. Ustione A, Piston DW. Dopamine synthesis and D3 receptor activation in pancreatic beta-cells regulates insulin secretion and intracellular [Ca(2+)] oscillations. Mol Endocrinol 2012; 26(11): 1928–1940. [PubMed: 22918877]
13. Garcia-Tornadu I, Ornstein AM, Chamson-Reig A, Wheeler MB, Hill DJ, Arany E et al. Disruption of the dopamine d2 receptor impairs insulin secretion and causes glucose intolerance. Endocrinology 2010; 151(4): 1441–1450. [PubMed: 20147524]
14. Rosati G, Maioli M, Aiello I, Farris A, Agnetti V. Effects of long-term L-dopa therapy on carbohydrate metabolism in patients with Parkinson's disease. European neurology 1976; 14(3): 229–239. [PubMed: 1278195]
15. Ericson LE, Hakanson R, Lundquist I. Accumulation of dopamine in mouse pancreatic B-cells following injection of L-DOPA. Localization to secretory granules and inhibition of insulin secretion. Diabetologia 1977; 13(2): 117–124. [PubMed: 404204]
16. Zern RT, Bird JL, Feldman JM. Effect of increased pancreatic islet norepinephrine, dopamine and serotonin concentration on insulin secretion in the golden hamster. Diabetologia 1980; 18(4): 341–346. [PubMed: 6998806]
17. Ustione A, Piston DW, Harris PE. Minireview: Dopaminergic regulation of insulin secretion from the pancreatic islet. Mol Endocrinol 2013; 27(8): 1198–1207. [PubMed: 23744894]
18. Moritz AE, Free RB, Sibley DR. Advances and challenges in the search for D2 and D3 dopamine receptor-selective compounds. Cell Signal 2018; 41: 75–81. [PubMed: 28716664]

19. Diaz-Torga G, Feierstein C, Libertun C, Gelman D, Kelly MA, Low MJ et al. Disruption of the D2 dopamine receptor alters GH and IGF-I secretion and causes dwarfism in male mice. Endocrinology 2002; 143(4): 1270–1279. [PubMed: 11897683]
20. Kelly MA, Rubinstein M, Asa SL, Zhang G, Saez C, Bunzow JR et al. Pituitary lactotroph hyperplasia and chronic hyperprolactinemia in dopamine D2 receptor-deficient mice. Neuron 1997; 19(1): 103–113. [PubMed: 9247267]
21. Wang GJ, Volkow ND, Fowler JS. The role of dopamine in motivation for food in humans: implications for obesity. Expert opinion on therapeutic targets 2002; 6(5): 601–609. [PubMed: 12387683]
22. Garcia-Tornadu I, Perez-Millan MI, Recouvreux V, Ramirez MC, Luque G, Risso GS et al. New insights into the endocrine and metabolic roles of dopamine D2 receptors gained from the Drd2 mouse. Neuroendocrinology 2010; 92(4): 207–214. [PubMed: 20975260]
23. Iturriza FC, Thibault J. Immunohistochemical investigation of tyrosine-hydroxylase in the islets of Langerhans of adult mice, rats and guinea pigs. Neuroendocrinology 1993; 57(3): 476–480. [PubMed: 8100618]
24. Persson-Sjogren S, Forsgren S, Taljedal IB. Tyrosine hydroxylase in mouse pancreatic islet cells, in situ and after syngeneic transplantation to kidney. Histol Histopathol 2002; 17(1): 113–121. [PubMed: 11813861]
25. Takayanagi M, Watanabe T. Immunocytochemical colocalizations of insulin, aromatic L-amino acid decarboxylase, dopamine beta-hydroxylase, S-100 protein and chromogranin A in B-cells of the chicken endocrine pancreas. Tissue & cell 1996; 28(1): 17–24. [PubMed: 8907725]
26. Ganic E, Johansson JK, Bennet H, Fex M, Artner I. Islet-specific monoamine oxidase A and B expression depends on MafA transcriptional activity and is compromised in type 2 diabetes. Biochem Biophys Res Commun 2015; 468(4): 629–635. [PubMed: 26546820]
27. Maffei A, Marie Segal A, Alvarez-Perez JC, Garcia-Ocana A, Harris P. Anti-incretin, anti-proliferative action of dopamine on beta-cells. Mol Endocrinol 2015: me20141273.
28. Merglen A, Theander S, Rubi B, Chaffard G, Wollheim CB, Maechler P. Glucose sensitivity and metabolism-secretion coupling studied during two-year continuous culture in INS-1E insulinoma cells. Endocrinology 2004; 145(2): 667–678. [PubMed: 14592952]
29. Romanova IV, Derkach KV, Mikhrina AL, Sukhov IB, Mikhailova EV, Shpakov AO. The Leptin, Dopamine and Serotonin Receptors in Hypothalamic POMC-Neurons of Normal and Obese Rodents. Neurochemical research 2018.
30. Newman AH, Grundt P, Cyriac G, Deschamps JR, Taylor M, Kumar R et al. N-(4-(4-(2,3-dichloro- or 2-methoxyphenyl)piperazin-1-yl)butyl)heterobiarylcarboxamides with functionalized linking chains as high affinity and enantioselective D3 receptor antagonists. Journal of medicinal chemistry 2009; 52(8): 2559–2570. [PubMed: 19331412]
31. Xiao J, Free RB, Barnaeva E, Conroy JL, Doyle T, Miller B et al. Discovery, optimization, and characterization of novel D2 dopamine receptor selective antagonists. Journal of medicinal chemistry 2014; 57(8): 3450–3463. [PubMed: 24666157]
32. Herrera PL. Adult insulin- and glucagon-producing cells differentiate from two independent cell lineages. Development 2000; 127(11): 2317–2322. [PubMed: 10804174]
33. Bello EP, Mateo Y, Gelman DM, Noain D, Shin JH, Low MJ et al. Cocaine supersensitivity and enhanced motivation for reward in mice lacking dopamine D2 autoreceptors. Nat Neurosci 2011; 14(8): 1033–1038. [PubMed: 21743470]
34. Jung MY, Skryabin BV, Arai M, Abbondanzo S, Fu D, Brosius J et al. Potentiation of the D2 mutant motor phenotype in mice lacking dopamine D2 and D3 receptors. Neuroscience 1999; 91(3): 911–924. [PubMed: 10391470]
35. Carter JD, Dula SB, Corbin KL, Wu R, Nunemaker CS. A practical guide to rodent islet isolation and assessment. Biological procedures online 2009; 11: 3–31. [PubMed: 19957062]
36. Livak KJ, Schmittgen TD. Analysis of relative gene expression data using real-time quantitative PCR and the 2(-Delta Delta C(T)) Method. Methods 2001; 25(4): 402–408. [PubMed: 11846609]
37. Feigin A, Fukuda M, Dhawan V, Przedborski S, Jackson-Lewis V, Mentis MJ et al. Metabolic correlates of levodopa response in Parkinson's disease. Neurology 2001; 57(11): 2083–2088. [PubMed: 11739830]

38. Aslanoglou D, George EW, Freyberg Z. Homogeneous Time-resolved Forster Resonance Energy Transfer-based Assay for Detection of Insulin Secretion. J Vis Exp 2018; (135).
39. Farino ZJ, Morgenstern TJ, Vallaghe J, Gregor N, Donthamsetti P, Harris PE et al. Development of a Rapid Insulin Assay by Homogenous Time-Resolved Fluorescence. PLoS One 2016; 11(2): e0148684. [PubMed: 26849707]
40. Li X, Wu X, Camacho R, Schwartz GJ, LeRoith D. Intracerebroventricular leptin infusion improves glucose homeostasis in lean type 2 diabetic MKR mice via hepatic vagal and non-vagal mechanisms. PLoS One 2011; 6(2): e17058. [PubMed: 21379576]
41. Zaafar DK, Zaitone SA, Moustafa YM. Role of metformin in suppressing 1,2-dimethylhydrazine-induced colon cancer in diabetic and non-diabetic mice: effect on tumor angiogenesis and cell proliferation. PLoS One 2014; 9(6): e100562. [PubMed: 24971882]
42. Matthews DR, Hosker JP, Rudenski AS, Naylor BA, Treacher DF, Turner RC. Homeostasis model assessment: insulin resistance and beta-cell function from fasting plasma glucose and insulin concentrations in man. Diabetologia 1985; 28(7): 412–419. [PubMed: 3899825]
43. Olofsson CS, Gopel SO, Barg S, Galvanovskis J, Ma X, Salehi A et al. Fast insulin secretion reflects exocytosis of docked granules in mouse pancreatic B-cells. Pflugers Archiv : European journal of physiology 2002; 444(1–2): 43–51. [PubMed: 11976915]
44. Barg S, Lindqvist A, Obermuller S. Granule docking and cargo release in pancreatic beta-cells. Biochemical Society transactions 2008; 36(Pt 3): 294–299. [PubMed: 18481945]
45. Feldman JM, Chapman B. Characterization of pancreatic islet monoamine oxidase. Metabolism: clinical and experimental 1975; 24(5): 581–588. [PubMed: 1092954]
46. Uchino H, Kanai Y, Kim DK, Wempe MF, Chairoungdua A, Morimoto E et al. Transport of amino acid-related compounds mediated by L-type amino acid transporter 1 (LAT1): insights into the mechanisms of substrate recognition. Mol Pharmacol 2002; 61(4): 729–737. [PubMed: 11901210]
47. Khunweeraphong N, Nagamori S, Wiriyasermkul P, Nishinaka Y, Wongthai P, Ohgaki R et al. Establishment of stable cell lines with high expression of heterodimers of human 4F2hc and human amino acid transporter LAT1 or LAT2 and delineation of their differential interaction with alpha-alkyl moieties. Journal of pharmacological sciences 2012; 119(4): 368–380. [PubMed: 22850614]
48. Camargo SM, Vuille-dit-Bille RN, Mariotta L, Ramadan T, Huggel K, Singer D et al. The molecular mechanism of intestinal levodopa absorption and its possible implications for the treatment of Parkinson's disease. J Pharmacol Exp Ther 2014; 351(1): 114–123. [PubMed: 25073474]
49. Sulzer D, Cragg SJ, Rice ME. Striatal dopamine neurotransmission: regulation of release and uptake. Basal ganglia 2016; 6(3): 123–148. [PubMed: 27141430]
50. Pivonello R, Ferone D, Lombardi G, Colao A, Lamberts SW, Hofland LJ. Novel insights in dopamine receptor physiology. European journal of endocrinology 2007; 156 Suppl 1: S13–21. [PubMed: 17413183]
51. Kongpracha P, Nagamori S, Wiriyasermkul P, Tanaka Y, Kaneda K, Okuda S et al. Structure-activity relationship of a novel series of inhibitors for cancer type transporter L-type amino acid transporter 1 (LAT1). Journal of pharmacological sciences 2017; 133(2): 96–102. [PubMed: 28242177]
52. Koller WC, Rueda MG. Mechanism of action of dopaminergic agents in Parkinson's disease. Neurology 1998; 50(6 Suppl 6): S11–14; discussion S44–18. [PubMed: 9633680]
53. Kostrzewa RM. Dopamine receptor supersensitivity. Neurosci Biobehav Rev 1995; 19(1): 1–17. [PubMed: 7770190]
54. Lopez Vicchi F, Luque GM, Brie B, Nogueira JP, Garcia Tornadu I, Becu-Villalobos D. Dopaminergic drugs in type 2 diabetes and glucose homeostasis. Pharmacological research 2016; 109: 74–80. [PubMed: 26748034]
55. Guo N, Guo W, Kralikova M, Jiang M, Schieren I, Narendran R et al. Impact of D2 Receptor Internalization on Binding Affinity of Neuroimaging Radiotracers. Neuropsychopharmacology 2010; 35(3): 806–817. [PubMed: 19956086]
56. Gangarossa G, Espallergues J, Mailly P, De Bundel D, de Kerchove d'Exaerde A, Herve D et al. Spatial distribution of D1R- and D2R-expressing medium-sized spiny neurons differs along the

rostro-caudal axis of the mouse dorsal striatum. Frontiers in neural circuits 2013; 7: 124. [PubMed: 23908605]

57. Armando I, Konkalmatt P, Felder RA, Jose PA. The renal dopaminergic system: novel diagnostic and therapeutic approaches in hypertension and kidney disease. Translational research : the journal of laboratory and clinical medicine 2015; 165(4): 505–511. [PubMed: 25134060]
58. Tayebati SK, Lokhandwala MF, Amenta F. Dopamine and vascular dynamics control: present status and future perspectives. Current neurovascular research 2011; 8(3): 246–257. [PubMed: 21722093]
59. Zhang MZ, Harris RC. Antihypertensive mechanisms of intra-renal dopamine. Current opinion in nephrology and hypertension 2015; 24(2): 117–122. [PubMed: 25594544]
60. Choi MR, Kouyoumdzian NM, Rukavina Mikusic NL, Kravetz MC, Roson MI, Rodriguez Fermepin M et al. Renal dopaminergic system: Pathophysiological implications and clinical perspectives. World journal of nephrology 2015; 4(2): 196–212. [PubMed: 25949933]
61. Wang X, Villar VA, Armando I, Eisner GM, Felder RA, Jose PA. Dopamine, kidney, and hypertension: studies in dopamine receptor knockout mice. Pediatric nephrology (Berlin, Germany) 2008; 23(12): 2131–2146.
62. Zeng C, Armando I, Luo Y, Eisner GM, Felder RA, Jose PA. Dysregulation of dopamine-dependent mechanisms as a determinant of hypertension: studies in dopamine receptor knockout mice. American journal of physiology Heart and circulatory physiology 2008; 294(2): H551–569. [PubMed: 18083900]
63. Morla L, Edwards A, Crambert G. New insights into sodium transport regulation in the distal nephron: Role of G-protein coupled receptors. World journal of biological chemistry 2016; 7(1): 44–63. [PubMed: 26981195]
64. Mitok KA, Freiberger EC, Schueler KL, Rabaglia ME, Stapleton DS, Kwiecien NW et al. Islet proteomics reveals genetic variation in dopamine production resulting in altered insulin secretion. J Biol Chem 2018.
65. Borelli MI, Rubio M, Garcia ME, Flores LE, Gagliardino JJ. Tyrosine hydroxylase activity in the endocrine pancreas: changes induced by short-term dietary manipulation. BMC endocrine disorders 2003; 3(1): 2. [PubMed: 12659644]
66. Vazquez P, Robles AM, de Pablo F, Hernandez-Sanchez C. Non-neural tyrosine hydroxylase, via modulation of endocrine pancreatic precursors, is required for normal development of beta cells in the mouse pancreas. Diabetologia 2014; 57(11): 2339–2347. [PubMed: 25082160]
67. Eisenhofer G, Kopin IJ, Goldstein DS. Catecholamine metabolism: a contemporary view with implications for physiology and medicine. Pharmacol Rev 2004; 56(3): 331–349. [PubMed: 15317907]
68. Cheng Q, Beltran VD, Chan SM, Brown JR, Bevington A, Herbert TP. System-L amino acid transporters play a key role in pancreatic beta-cell signalling and function. Journal of molecular endocrinology 2016; 56(3): 175–187. [PubMed: 26647387]
69. Carranza A, Musolino PL, Villar M, Nowicki S. Signaling cascade of insulin-induced stimulation of L-dopa uptake in renal proximal tubule cells. American journal of physiology Cell physiology 2008; 295(6): C1602–1609. [PubMed: 18842830]
70. Eldrup E, Moller SE, Andreasen J, Christensen NJ. Effects of ordinary meals on plasma concentrations of 3,4-dihydroxyphenylalanine, dopamine sulphate and 3,4-dihydroxyphenylacetic acid. Clinical science (London, England : 1979) 1997; 92(4): 423–430.
71. Eldrup E, Richter EA. DOPA, dopamine, and DOPAC concentrations in the rat gastrointestinal tract decrease during fasting. Am J Physiol Endocrinol Metab 2000; 279(4): E815–822. [PubMed: 11001763]
72. Goldstein DS, Eisenhofer G, Kopin IJ. Sources and significance of plasma levels of catechols and their metabolites in humans. J Pharmacol Exp Ther 2003; 305(3): 800–811. [PubMed: 12649306]
73. Goldstein DS, Swoboda KJ, Miles JM, Coppack SW, Aneman A, Holmes C et al. Sources and physiological significance of plasma dopamine sulfate. The Journal of clinical endocrinology and metabolism 1999; 84(7): 2523–2531. [PubMed: 10404831]

74. Eldrup E, Richter EA, Christensen NJ. DOPA, norepinephrine, and dopamine in rat tissues: no effect of sympathectomy on muscle DOPA. The American journal of physiology 1989; 256(2 Pt 1): E284–287. [PubMed: 2493196]

75. Beaulieu JM, Espinoza S, Gainetdinov RR. Dopamine receptors - IUPHAR Review 13. British journal of pharmacology 2015; 172(1): 1–23. [PubMed: 25671228]

76. Leggio GM, Bucolo C, Platania CB, Salomone S, Drago F. Current drug treatments targeting dopamine D3 receptor. Pharmacol Ther 2016; 165: 164–177. [PubMed: 27343365]

77. Newman AH, Beuming T, Banala AK, Donthamsetti P, Pongetti K, LaBounty A et al. Molecular determinants of selectivity and efficacy at the dopamine D3 receptor. Journal of medicinal chemistry 2012; 55(15): 6689–6699. [PubMed: 22632094]

78. Ford CP. The role of D2-autoreceptors in regulating dopamine neuron activity and transmission. Neuroscience 2014; 282: 13–22. [PubMed: 24463000]

79. Mims RB, Scott CL, Modebe OM, Bethune JE. Prevention of L-dopa-induced growth hormone stimulation by hyperglycemia. The Journal of clinical endocrinology and metabolism 1973; 37(5): 660–663. [PubMed: 4749441]

80. Sandyk R The relationship between diabetes mellitus and Parkinson's disease. The International journal of neuroscience 1993; 69(1–4): 125–130. [PubMed: 8082998]

81. Furman BL, Wilson GA. The effects of levodopa on plasma glucose in two strains of rat. Eur J Pharmacol 1979; 55(3): 241–246. [PubMed: 456422]

82. Hahn M, Chintoh A, Giacca A, Xu L, Lam L, Mann S et al. Atypical antipsychotics and effects of muscarinic, serotonergic, dopaminergic and histaminergic receptor binding on insulin secretion in vivo: an animal model. Schizophr Res 2011; 131(1–3): 90–95. [PubMed: 21696923]

83. Lako IM, van den Heuvel ER, Knegtering H, Bruggeman R, Taxis K. Estimating dopamine D(2) receptor occupancy for doses of 8 antipsychotics: a meta-analysis. Journal of clinical psychopharmacology 2013; 33(5): 675–681. [PubMed: 23948784]

84. Kopf D, Gilles M, Paslakis G, Medlin F, Lederbogen F, Lehnert H et al. Insulin secretion and sensitivity after single-dose amisulpride, olanzapine or placebo in young male subjects: double blind, cross-over glucose clamp study. Pharmacopsychiatry 2012; 45(6): 223–228. [PubMed: 22426845]

85. Teff KL, Rickels MR, Grudziak J, Fuller C, Nguyen HL, Rickels K. Antipsychotic-induced insulin resistance and postprandial hormonal dysregulation independent of weight gain or psychiatric disease. Diabetes 2013; 62(9): 3232–3240. [PubMed: 23835329]

86. Kowalchuk C, Castellani L, Chintoh A, Remington G, Giacca A, Hahn M. Antipsychotics and glucose metabolism: how brain and body collide. Am J Physiol Endocrinol Metab 2018.

87. Hahn MK, Wolever TM, Arenovich T, Teo C, Giacca A, Powell V et al. Acute effects of single-dose olanzapine on metabolic, endocrine, and inflammatory markers in healthy controls. Journal of clinical psychopharmacology 2013; 33(6): 740–746. [PubMed: 24100786]

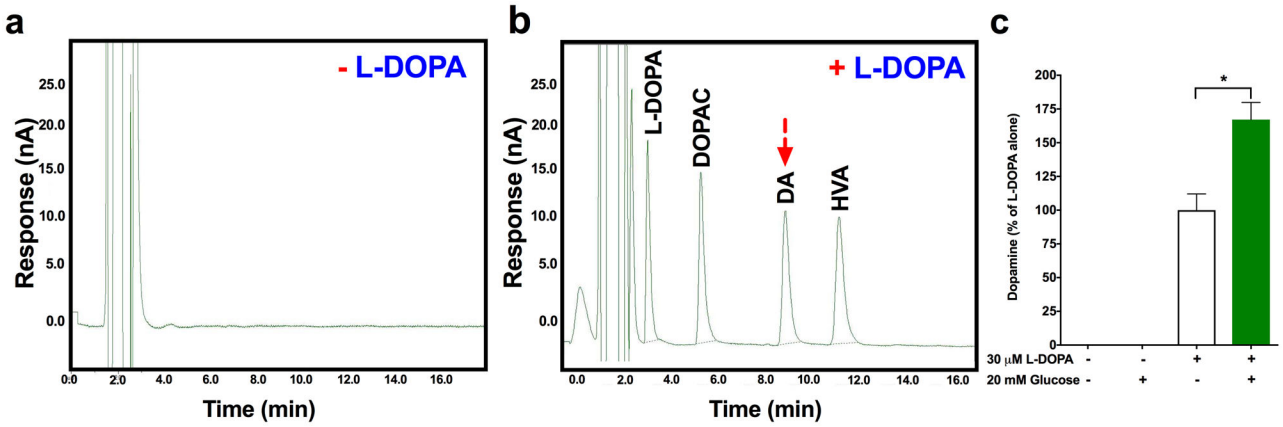

Figure 1. Insulin-secreting INS-1E cells require the dopamine precursor L-DOPA for dopamine biosynthesis and release.

(a) Representative high-performance liquid chromatography (HPLC) traces of secreted dopamine (DA) and its metabolites from INS-1E cells. There was no detectable DA or DA metabolites (HVA, DOPAC) in the absence of supplementation with the DA precursor L-DOPA. **(b)** Representative HPLC trace showing that pre-incubation with L-DOPA (30 μM, 90 min, 37°C) led to detection of secreted DA and its metabolites, DOPAC and HVA. All analyses were performed in triplicate from n>3 independent experiments. **(c)** HPLC analysis of glucose-stimulated DA secretion from INS-1E cells pre-incubated with 30 μM L-DOPA. Glucose stimulation (20 mM, 90 min, 37°C) increased secreted DA by 70% compared to the unstimulated condition (P=0.013). Results were normalized to mean DA secretion in the non-glucose stimulated condition. Analyses were performed in triplicate from n≥9 independent experiments. All experiments were performed in triplicate from n≥3 independent experiments. For **c**, all bars represent the mean ± SEM. *P<0.05

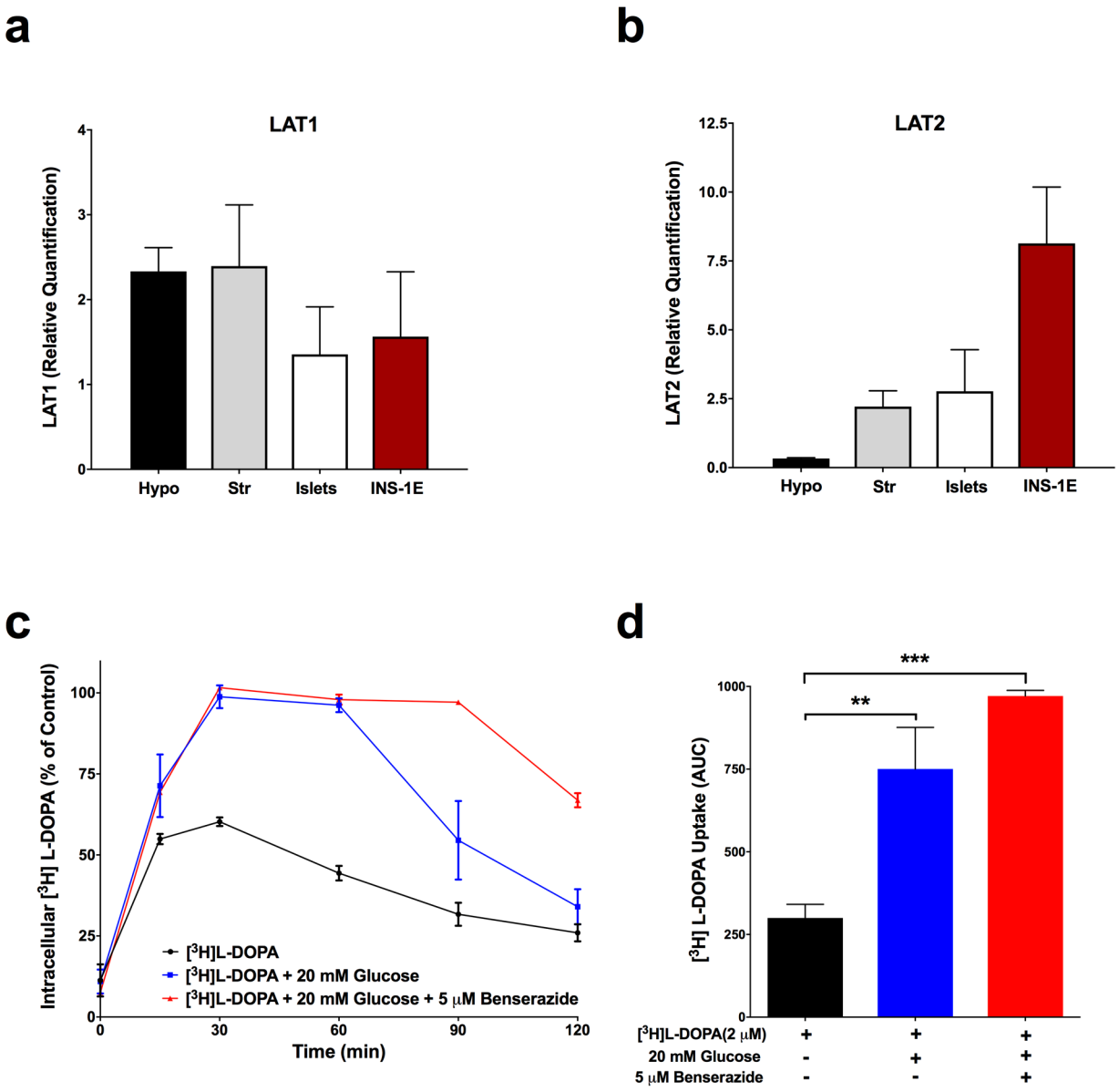

Figure 2. Glucose stimulation enhances L-DOPA uptake in INS-1E cells.

(a-b) Comparative qPCR analysis of L-type amino acid transporter 1 (LAT1) and −2 (LAT2) mRNA transcripts in INS-1E cells as well as from wildtype C57BL/6J mouse pancreatic islets, hypothalamus and striatum (n=4 for all groups). LAT1 mRNA levels were comparable between all groups ($P>0.05$). LAT2 mRNA was present in all groups (n=3–4), though highest in INS-1E cells [$F(3,11)=7.154$, $P=0.0062$]. Results are reported as the relative copy number of each transcript normalized to expression levels of *Rplp0*. **(c)** Time course of [^{3}H]L-DOPA (2 μM) uptake in the presence (blue square) or absence (black circle) of 20 mM glucose stimulation. Glucose stimulation caused a 40% increase in [^{3}H]L-DOPA uptake within 30 min relative to the unstimulated condition ($P=0.0005$). The AADC inhibitor benserazide (5 μM, red triangle) inhibited decreases in [^{3}H]L-DOPA accumulation at later time points (60–120 min). Data was normalized to the point of maximal [^{3}H]L-DOPA

uptake. Error bars indicate SEM. **(d)** Area under the curve (AUC) analysis of [^{3}H]L-DOPA uptake for the 3 conditions shown in **c**. Glucose stimulation caused a significant overall AUC change [F(2,5)=42.72, P=0.001]. There was a 2.5-fold increase in the glucose-stimulated condition compared to the unstimulated condition (P=0.002). Benserazide (5 μM) addition further enhanced this AUC increase (P=0.001). For **a-d**, measurements were performed in triplicate and represent the mean of n≥3 independent experimental days. For **a**,**b** and **d**, all bars represent the mean ± SEM. **P<0.01, ***P<0.001.

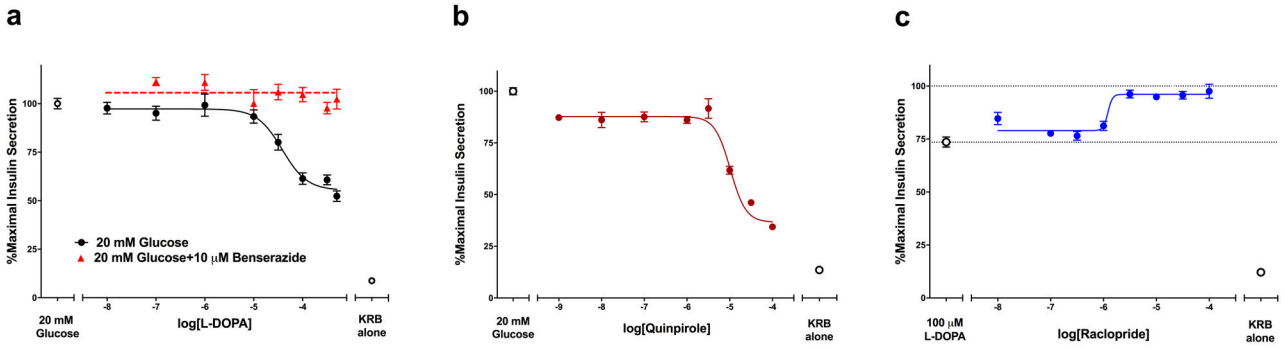

Figure 3. Effects of L-DOPA and D2R/D3R blockade on glucose-stimulated insulin secretion.

HTRF-based measurement of secreted insulin in INS-1E cells in response to 20 mM glucose stimulation (90 min, 37°C). **(a)** Increasing concentrations of L-DOPA caused dose-dependent inhibition of GSIS, which was best fit to a sigmoidal curve (in black; IC_{50}=38.3 μM, R^{22}=0.84). AADC inhibition by benserazide (10 μM) abolished L-DOPA's inhibition of GSIS (in red). **(b)** Treatment with the D2R/D3R agonist quinpirole produced a dose-dependent inhibition of GSIS (in black; IC_{50}=10.3 μM, R^{22}=0.90) **(c)** Concurrent blockade of D2R and D3R by increasing concentrations of raclopride in the presence of 100 μM L-DOPA attenuated L-DOPA's inhibitory effects on GSIS. Dotted lines indicate the minimum and maximum values constituting the dynamic range of the dose response curve. Results are represented as % maximal insulin secretion based on mean HTRF values from experiments performed in triplicate in n≥3 independent experiments. All values represent the mean ± SEM.

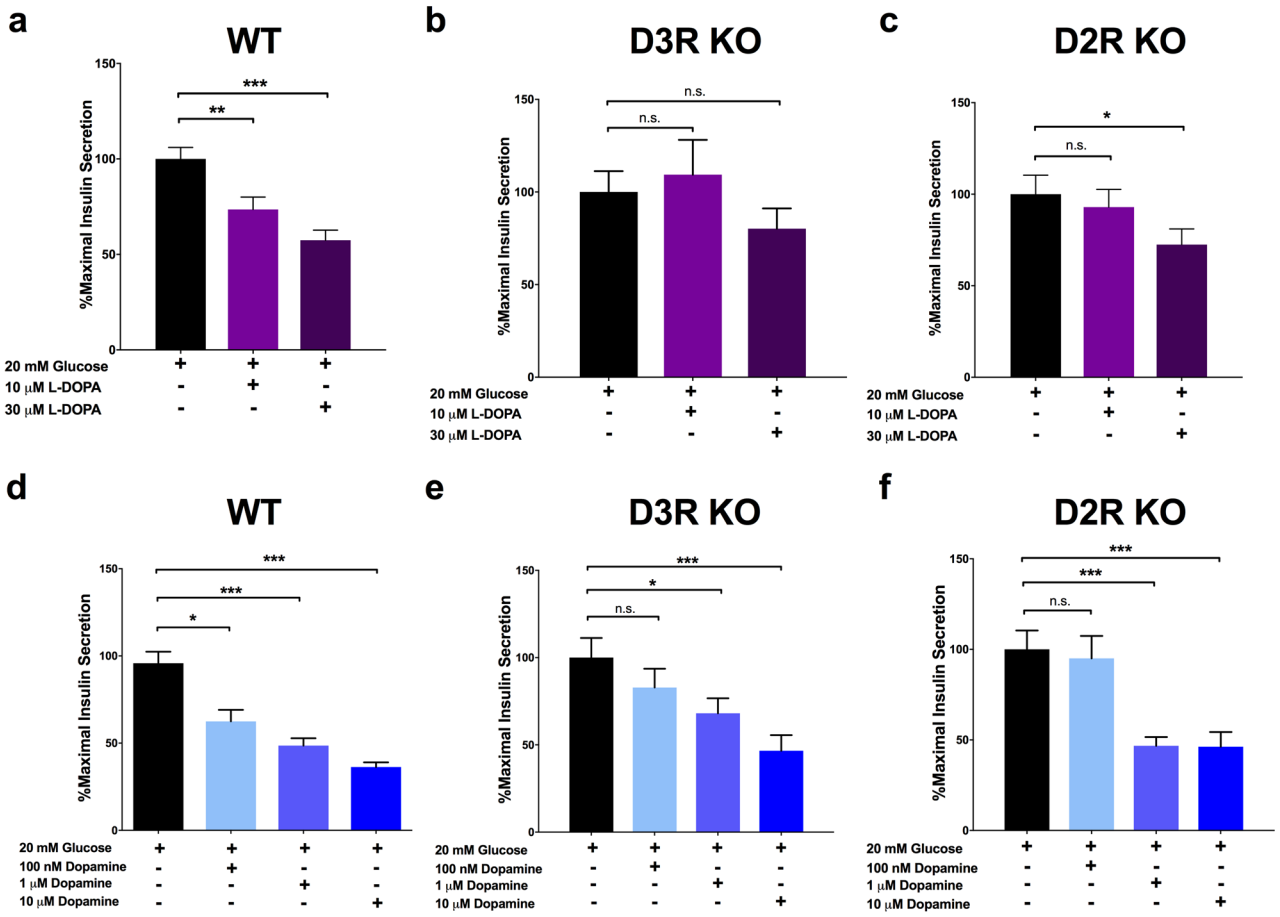

Figure 4. Effects of L-DOPA and dopamine on glucose-stimulated insulin secretion in pancreatic islets of D2R or D3R knockout mice.

(a) L-DOPA treatment significantly inhibited glucose-stimulated insulin secretion (GSIS) in pancreatic islets from wildtype (WT) C57BL/6J mice in a concentration-dependent manner [$F(2,67)=12.32$, $P<0.0001$]. GSIS was reduced both with 10 μM L-DOPA ($p=0.006$), and 30 μM L-DOPA ($P<0.0001$) compared to stimulation with 20 mM glucose alone (n=20 for all groups). **(b)** Inhibitory effects of L-DOPA on GSIS were attenuated in pancreatic islets from homozygous global D3R KO mice at both 10 μM and 30 μM L-DOPA concentrations [$F(2,42)=1.12$, $P>0.05$, n=15 for all groups]. **(c)** While no significant GSIS inhibition was evident at 10 μM L-DOPA ($P>0.05$), and largely attenuated at 30 μM L-DOPA ($P=0.05$; n=16 for all groups) in islets from β-cell-selective D2R KO mice. **(d)** DA treatment of pancreatic islets from WT mice significantly inhibited GSIS in a dose-dependent manner compared to stimulation with 20 mM glucose alone [$F(3,74)=13.11$, $P<0.001$] (100 nM: $P=0.026$; 1 μM: $P<0.0001$; 10 μM: $P<0.0001$; n=35 for all groups). **(e)** Pancreatic islets from global D3R KO mice exhibited significant DA-induced GSIS inhibition [$F(3,56)=5.17$, $P=0.003$]. Though D3R KO islets did not significantly respond to 100 nM DA, both 1 μM DA ($P=0.03$), and 10 μM DA treatment significantly inhibited GSIS ($P=0.001$; n=15 for all groups). **(f)** Pancreatic islets from β-cell-specific D2R KO mice responded to DA treatment [$F(3,60)=6.60$, $P=0.001$]. D2R KO islets exhibited GSIS inhibition at higher DA concentrations: 1 μM ($P<0.0001$) and 10 μM DA ($P=0.0003$), but not at 100 nM DA

(P>0.05; n=16 for all groups). Results are represented as % maximal insulin secretion based on mean HTRF values from n≥6 replicate samples in age-matched mice. Assays were conducted on n≥3 independent experimental days. All bars represent the mean ± SEM. *P<0.05, **P<0.01, ***P<0.001.

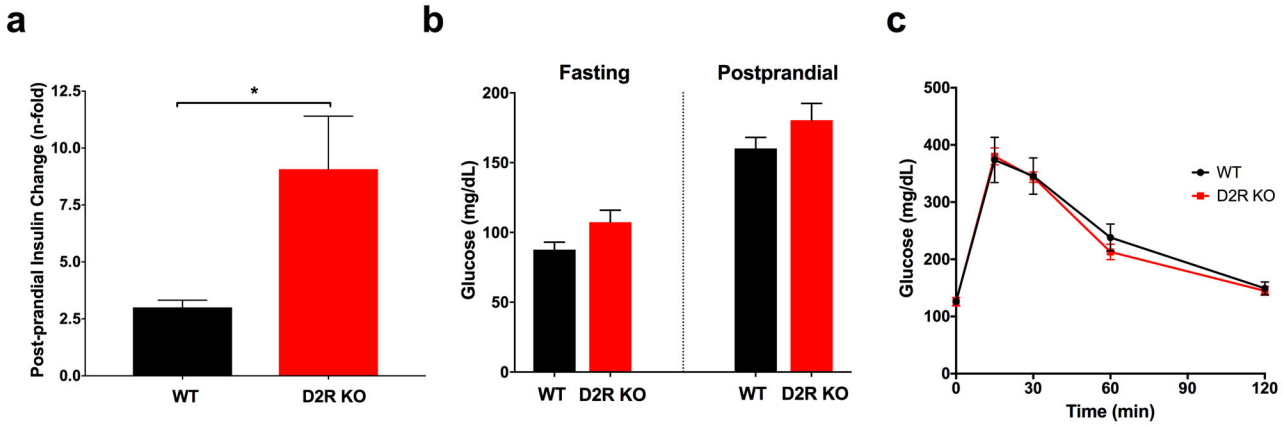

Figure 5. Glucose-stimulated DA secretion is reduced in D2R and D3R KO pancreatic islets.

(a) Postprandial elevation in serum insulin levels was 3-fold higher in homozygous pancreatic β-cell-selective D2R KO mice (n=12) compared to WT littermate controls (n=9; P=0.038). Postprandial serum insulin values were normalized to subjects' respective pre-meal fasting serum insulin levels. Assays were conducted in triplicate on n≥3 independent experimental days. **(b)** There were no significant differences in either pre-meal fasting or postprandial glucose levels between homozygous pancreatic β-cell-selective D2R KO mice (n=12) compared to WT littermate controls (n=9; P>0.05). **(c)** Intraperitoneal glucose tolerance test (ipGTT, 2 g/kg). There were no significant differences in glucose tolerance between homozygous pancreatic β-cell-selective D2R KO mice (n=6) compared to WT littermate controls (n=10; P>0.05). All bars and points represent the mean ± SEM. *P<0.05.